JACS
JOURNAL OF THE AMERICAN CHEMICAL SOCIETY
Article
pubs.acs.org/JACS

Formation of Ethane from Mono-Methyl Palladium(II) Complexes

Monica D. Lotz,[†] Matthew S. Remy,[†] David B. Lao,[‡] Alireza Ariafard,[§] Brian F. Yates,[§] Allan J. Canty,*[,§] James M. Mayer,[‡] and Melanie S. Sanford*[,†]

[†]Department of Chemistry, University of Michigan, 930 North University Avenue, Ann Arbor, Michigan 48109, United States
[‡]Department of Chemistry, University of Washington, Box 351700, Seattle, Washington 98195, United States
[§]School of Chemistry, University of Tasmania, Private Bag 75, Hobart, Tasmania 7001, Australia

Supporting Information

ABSTRACT: This article describes the high-yielding and selective oxidatively induced formation of ethane from mono-methyl palladium complexes. Mechanistic details of this reaction have been explored via both experiment and computation. On the basis of these studies, a mechanism involving methyl group transmetalation between Pd^{II} and Pd^{IV} interedíates is proposed.

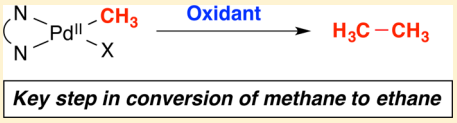

INTRODUCTION

The catalytic oxidative coupling of methane is an attractive route to ethane and higher hydrocarbons.[1] While heterogeneous catalysts are known for this transformation,[1,2] their modest selectivities and high reaction temperatures have motivated the pursuit of more selective and milder homogeneous alternatives.[3] To date, examples of homogeneous catalytic alkane/alkane coupling remain rare.[4,5] We hypothesized that the development of such processes could be informed by analogy to better-known arene C–H oxidative coupling reactions.[6] For instance, the Pd-catalyzed dimerization of dimethyl phthalate is a key step in the industrial preparation of the monomer precursor to Upilex.[7] The catalytic cycle for this reaction is believed to involve the following steps: (*i*) arene C–H activation by **A** to generate mono-aryl Pd^{II} complex $\mathbf{B_{Ar}}$ (Ar = aryl), (*ii*) disproportionation to form bis-aryl Pd^{II} adduct $\mathbf{C_{Ar}}$, (*iii*) C–C bond-forming reductive elimination to release the product biaryl and Pd^0, and (*iv*) oxidation of Pd^0 to regenerate the Pd^{II} catalyst (Scheme 1).

Scheme 1. Pd-Catalyzed Arene Oxidative Dimerization

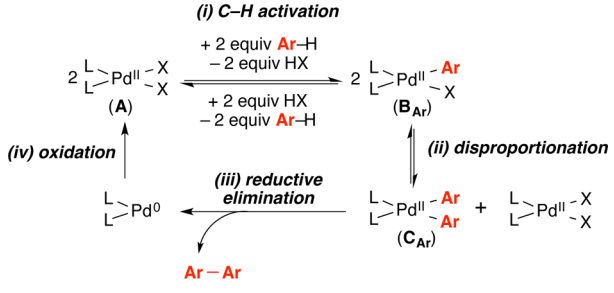

Methane activation at Pd^{II} to form mono-methyl complexes analogous to $\mathbf{B_{Ar}}$ has significant precedent.[5,8,9] In contrast, the generation of ethane from analogues of $\mathbf{B_{Ar}}$ (putative steps *ii* and *iii*) has not been reported.[10] The primary challenges associated with ethane formation from mono-methyl Pd^{II} complexes are that (a) transmetalation at Pd^{II} (step *ii*) is highly thermodynamically unfavorable[11] and (b) the subsequent C–C coupling step at dimethyl Pd^{II} complexes is slow and low yielding, even under forcing conditions.[11] We hypothesized that these challenging steps could be circumvented via the catalytic cycle proposed in Scheme 2. This would involve: (*i*) CH_4 activation at Pd^{II} to generate mono-methyl complex $\mathbf{B_{Me}}$, (*ii*) oxidatively induced transmetalation to form dimethyl Pd^{IV} species **D**, and (*iii*) C–C coupling from **D** to regenerate the Pd^{II} catalyst.[7]

Scheme 2. Proposed Catalytic Cycle for Pd-Catalyzed Methane Oxidative Dimerization

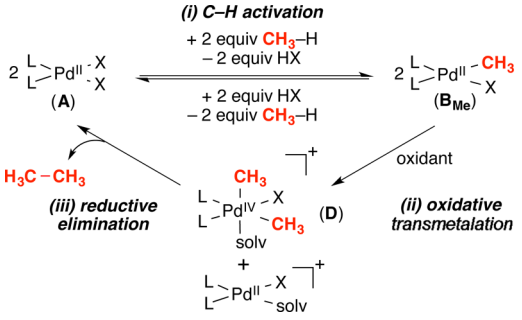

Importantly, CH_3–CH_3 coupling at Pd^{III} and Pd^{IV} dimethyl complexes (step *iii*) is well-known to occur much more readily than that from analogous Pd^{II} species.[3c,10,12,13] Furthermore, we have previously demonstrated a related oxidatively induced CH_3–CH_3 reductive elimination starting with the dimethyl Pd^{II} complex (dtbpy)$Pd(CH_3)_2$ (**1**, dtbpy = 4,4′-di-*tert*-butyl-2,2′-bipyridine) (eq 1).[3a] The treatment of **1** with 1.1 equiv of ferrocenium (Fc^+) yielded ethane in 49% yield (maximum theoretical yield = 50%) via Pd^{IV} intermediate **2**. This reaction provides proof-of-principle for the feasibility of the proposed oxidative transmetalation step (Scheme 2, step *ii*). However,

Received: December 10, 2013

   dx.doi.org/10.1021/ja412338k | J. Am. Chem. Soc. XXXX, XXX, XXX–XXX

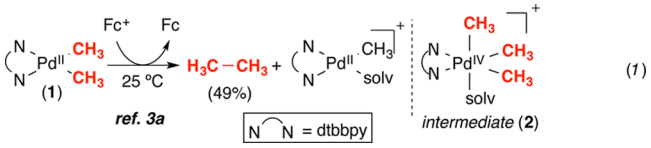

(1)

there is currently no precedent for accessing Pd dimethyl complexes like **1** via CH_4 activation.[14] *Thus, in order to realize the catalytic cycle in Scheme 2, it is critical to achieve CH_3–CH_3 coupling from mono-methyl intermediates like B_{Me}.*[9] Herein, we report oxidatively induced ethane formation from mono-methyl Pd^{II} complexes. Both experimental and computational details about the mechanism of this transformation are discussed.

RESULTS AND DISCUSSION

Reactivity of 3. Our initial studies focused on the generation of ethane from mono-methyl Pd^{II} complex (dtbpy)Pd(CH_3)(OAc) (**3**). Acetate and other carboxylate ligands have been widely utilized in Pd-catalyzed methane functionalization reactions.[9,15] These are often proposed to promote C–H activation via concerted metalation–deprotonation-type mechanisms.[16] Complex **3** was synthesized by the reaction of (dtbpy)Pd^{II}(CH_3)(Cl) with AgOAc and was characterized by NMR spectroscopy and elemental analysis. This complex is quite stable in the absence of an oxidant. For instance, it can be stored in the solid state at −33 °C for several months without detectable decomposition. It is also stable in acetone at room temperature under N_2 for at least 24 h. Complex **3** does decompose upon heating to 100 °C for 21 h in acetone-d_6 (eq 2). This results in CH_3D as the major organic product (83% yield) along with only small amounts of ethane (7%). Notably, no CH_3OAc was observed under these thermolysis conditions.

(2)

In contrast, **3** reacts rapidly with various oxidants at 25 °C in acetone-d_6 to form ethane in 11–37% yield (Table 1).

Table 1. Oxidation of 3 with $1e^-$ and $2e^-$ Oxidants[a]

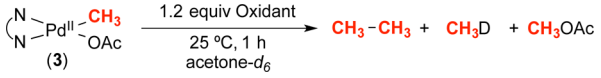

entry	oxidant	yield C_2H_6[b]	yield CH_4[c]	yield CH_3OAc
1	$K_2S_2O_8$	11%	<1%	<1%
2	$PhI(OAc)_2$	15%	31%	37%
3	$PhI(OTFA)_2$	28%	3%	49%[d]
4	CAN	17%	<1%	<1%
5	$AgBF_4$	22%	1%	<1%
6	$AcFcBF_4$	36%	<1%	<1%
7	NFTPT	31%	<1%	<1%
8[e]	NFTPT	37%	1%	<1%

[a]Conditions: **3** (4 μmol, 1 equiv), oxidant (4.8 μmol, 1.2 equiv), 1,1,2-trichloroethane (4 μmol, 1 equiv, standard), acetone-d_6, 25 °C, 24 h. [b]The theoretical maximum yield of ethane is 50%. [c]The theoretical maximum yield of CH_4 and CH_3OAc is 100%. [d]CH_3OTFA is formed in 49% yield in this reaction. [e]Conditions: **3** (4 μmol, 1 equiv), NFTPT (20 μmol, 5 equiv), 1,1,2-trichloroethane (4 μmol, 1 equiv, standard), acetone-d_6, 25 °C, 1 h.

Importantly, the maximum possible yield of ethane in these experiments is 50%. Minimal CH_3D (or CH_4) is observed with most oxidants (≤1% in all cases except with hypervalent iodine oxidants, entries 2 and 3). The yield of ethane varies significantly as a function of oxidant. In some cases, this is due to competitive processes. For instance, hypervalent iodine oxidants bearing carboxylate ligands (e.g., $PhI(OAc)_2$, $PhI(OTFA)_2$, entries 2 and 3) afford significant quantities of CH_3OAc and CH_3OTFA as well as CH_3D. Overall, the highest yields of ethane (and cleanest reactions) are observed with the $1e^-$ oxidant acetylferrocenium tetrafluoroborate ($AcFcBF_4$)[17] and the $2e^-$ oxidant *N*-fluoropyridinium triflate (NFTPT) (entries 6 and 7). The reaction of **3** with 1.2 equiv of each of these oxidants affords ethane in 36 and 31% yield, respectively. With 1.2 equiv of NFTPT, there was ∼15% of a Pd(CH_3) species remaining at the end of this reaction. The use of an excess of oxidant (5 equiv) could be used to push the reaction to full conversion; under these conditions, ethane was formed in 37% yield (entry 8).

The inorganic byproducts of these transformations are (dtbpy)Pd^{II}(OAc)(BF_4) (**4**) with $AcFcBF_4$ and (dtbpy)Pd^{II}(OAc)$(X)^+$ [X = F^- (**5-F**); X = 2,4,6-trimethylpyridine (**5-TP**)] with NFTPT. The X ligands of **4** and **5** (BF_4^-, F^-, and TP) are in rapid exchange with solvent (acetone or water); thus, the complexes were converted to the corresponding iodide salts to determine yields. This procedure established that the yield of **4** is 43% and the yield of **5-F**/**TP** is 55% under our standard reaction conditions.

Mechanistic Studies. We next sought to gain insights into the mechanism of ethane formation in these systems using a combination of experiment and theory. A first set of experiments was performed to assess whether methyl radical intermediates (CH_3•) are involved in ethane formation from complex **3**. The reactions of **3** with $AcFcBF_4$ and NFTPT were performed in the presence of 40 equiv of the H atom donor 1,4-cyclohexadiene (CHD). As discussed in our prior work,[3a] CH_3• intermediates formed under these conditions would be expected to participate in rapid H• abstraction from cyclohexadiene to afford CH_4 in high yield. As shown in Table 2, entries 3 and 4, ≤6% methane was detected under these conditions, with only small decreases in the yield of ethane. These results suggest against CH_3• formation as a major pathway to

Table 2. Influence of Cyclohexadiene and Light of Oxidative Ethane Formation from 3[a]

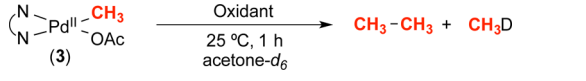

entry	oxidant	conditions	yield C_2H_6	yield CH_4
1	$AcFcBF_4$	none	36%	<1%
2	NFTPT	none	37%	1%
3[b]	$AcFcBF_4$	CHD	29%	2%
4[b]	NFTPT	CHD	35%	6%
5[c]	$AcFcBF_4$	no light	38%	<1%
6[c]	NFTPT	no light	39%	<1%

[a]Conditions: **3** (4 μmol, 1 equiv), $AcFcBF_4$ (4.8 μmol, 1.2 equiv) or NFTPT (20 μmol, 5 equiv), 1,1,2-trichloroethane (4 μmol, 1 equiv, standard), acetone-d_6, 25 °C, 1 h. [b]40 mmol of 1,4-cyclohexadiene (CHD) added under the standard conditions. [c]Reaction conducted under standard conditions but in a foil-wrapped NMR tube to exclude ambient light.

dx.doi.org/10.1021/ja412338k | J. Am. Chem. Soc. XXXX, XXX, XXX–XXX

ethane. We also compared the reactions of **3** with $AcFcBF_4$ and NFTPT carried out under ambient light to those conducted in foil-wrapped NMR tubes. As shown in entries 5 and 6, nearly identical yields were obtained in the presence and absence of light, suggesting against mechanisms involving light-induced cleavage of the Pd−CH_3 bonds.

We next conducted low temperature NMR experiments in an attempt to observe organometallic intermediates during the oxidation of complex **3**. Importantly, our previous studies of the reaction of Pd dimethyl complex **1** with $FcBF_4$ showed the formation of trimethyl Pd^{IV} intermediate **2** (eq 1).[3a] Complex **2** was proposed to form via initial oxidation of **1** followed by subsequent methyl group transmetalation between a dimethyl Pd^{IV} intermediate and the dimethyl Pd^{II} starting material. Intermediate **2** is stabilized by the presence of three strongly electron donating methyl groups; thus, its detection at low temperature by ^1H NMR spectroscopy was relatively straightforward.[12]

We hypothesized that an analogous methyl group transmetalation process could be occurring during the oxidation of **3** (Scheme 3). However, here, the penultimate organometallic

Scheme 3. Proposed Mechanism for Ethane Formation from 3

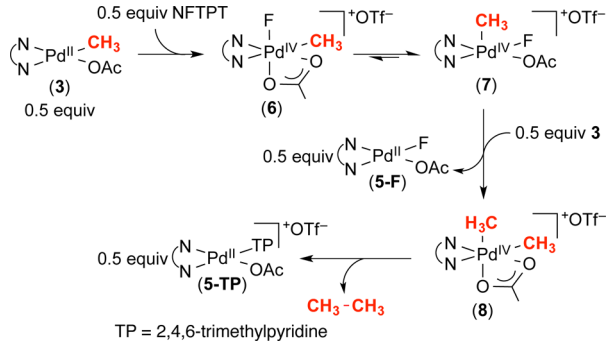

intermediate would be the dimethyl Pd^{IV} species **8**, which is expected to be significantly less stable than its trimethyl analogue.[12] The treatment of **3** with NFTPT or $AcFcBF_4$ at −78 °C in CD_2Cl_2 resulted in ^1H NMR spectra with broad, uninterpretable signals. The formation of ethane occurred upon warming these samples to −60 °C. The addition of 100 equiv of CH_3CN (which was anticipated to stabilize cationic Pd^{IV} complexes such as **8**)[12] did marginally enhance the stability of the intermediates formed during this process. However, the spectra remained broad and showed a complex mixture of ^1H NMR signals. Furthermore, warming this mixture to −40 °C resulted in the rapid liberation of ethane.

We turned to DFT to obtain a mechanistic picture of the reactivity of **3** with oxidants. We selected the reaction of NFTPT with **3** for detailed computational study for two reasons. First, it affords the highest yield of ethane of any of the transformations in Table 1. Second, NFTPT is well-known to function as a $2e^-$ oxidant for Pd^{II} centers,[18] thus limiting the likelihood of odd-electron intermediates, which would be much more difficult to treat computationally.[19] Notably, these calculations were performed using bipyridine (bpy) in place of dtbpy as the ligand at palladium; as such, the starting material is termed **3′** and subsequent intermediates are denoted with a prime. The DFT calculations[20] show a low energy $2e^-$ oxidation path that has three steps in the overall conversion of **3′** + NFTP (*N*-fluoropyridinium) to **5′-F**/**5′-TP** and ethane. These steps are (1) oxidation of 0.5 equiv of **3′** by NFTP to generate Pd^{IV} isomers **6′** and **7′**, (2) methyl group transmetalation between 1 equiv of **7′** and 1 equiv of Pd^{II} starting material **3′** to form **8′** and **5-F′**,[19,20] and (3) ethane reductive elimination from **8′** to release the products. The details of each step are discussed below. The initial oxidation of **3′** with NFTP proceeds via **TS_I′** (Figure 1) with transfer of F^+ to the Pd center. This activation barrier ($\Delta G^{\ddagger}$ = 17.6 kcal/mol) is the highest for the entire sequence. The initial product **6′** isomerizes to **7′** via a transition structure (**TS_II′**) with a very low barrier, as would be anticipated for a labile five-coordinate Pd^{IV} center.[12] The isomerization is highly thermodynamically favorable (ΔG = −8.7 kcal/mol).

Transmetalation of the methyl ligand between **3′** and **7′** proceeds via an early transition state in which the transferring methyl group is much closer to the initial Pd^{IV} than the incoming Pd^{II} nucleophile, as reflected in the Pd−CH_3 distances (2.183 and 2.756 Å, respectively, in **TS_III′**). The geometry at the carbon of the bridging methyl ligand is not quite trigonal bipyramidal, as reflected in CH_2 angles (117.4−117.9°). The transition structure shows a single imaginary frequency, with an "umbrella" motion for the methyl group. The transmetalation reaction is thermodynamically downhill (ΔG = −19.8 kcal/mol) and is essentially barrierless. The transmetalation process is facilitated by the excellent orbital match between the HOMO of **3′** and the LUMO of **7′** (Figure 1).

Finally, ethane formation occurs via H_3C-CH_3 coupling at the five-coordinate complex **8′** (containing an additional weak Pd···O interaction). The barrier for this process is calculated to be low (10.5 kcal/mol) in the absence of a strongly coordinating ligand to fill the sixth coordination site. The other possible reductive elimination reaction from **8′** (H_3C-OAc coupling) is much less favorable, with a barrier of 32.4 kcal/mol. This is consistent with the fact that this product is not observed with NFTPT as the oxidant.

Model Complex to Detect Intermediates. We reasoned that replacing the OAc of **3** with a more stabilizing X-type ligand might enable detection of some of the short-lived intermediates in this ethane-forming reaction. Several recent reports have shown that CF_3 ligands stabilize related Pd^{IV} intermediates.[18b,c,d,21] Furthermore, CF_3 ligands are notoriously inert in reductive elimination reactions, suggesting the possibility that methyl ligand transmetalation between Pd centers could outcompete reductive elimination to form F_3C-CH_3. Thus, we next targeted (dtbpy)$Pd^{II}(CH_3)(CF_3)$ (**9**) as a model compound for probing reaction intermediates and mechanisms of oxidatively induced ethane formation from mono-methyl Pd complexes.

Complex **9** was prepared by treating (tmeda)$Pd^{II}(CH_3)(I)$ with CsF/$TMSCF_3$ and then dtbpy. It was characterized by NMR spectroscopy and elemental analysis. Palladium(II) complex **9** is even more stable than **3** in the absence of oxidants. It can be stored under N_2 in the solid state for >6 months without detectable decomposition and is stable at 25 °C in acetone for at least 2 days under N_2. Even at 100 °C in acetone, it only decomposes completely after 8 days, yielding CH_3D as the major organic product in 74% yield. Trace ethane (<5%) and no F_3C-CH_3 were detected (eq 3).

Complex **9** reacts rapidly with $AcFcBF_4$ and NFTPT at 25 °C in acetone-d_6 to afford ethane in 34 and 41% yield, respectively (Table 3, entries 1 and 2). As with complex **3**, ≤2% yield of methane was detected in these reactions. The inorganic

dx.doi.org/10.1021/ja412338k | J. Am. Chem. Soc. XXXX, XXX, XXX−XXX

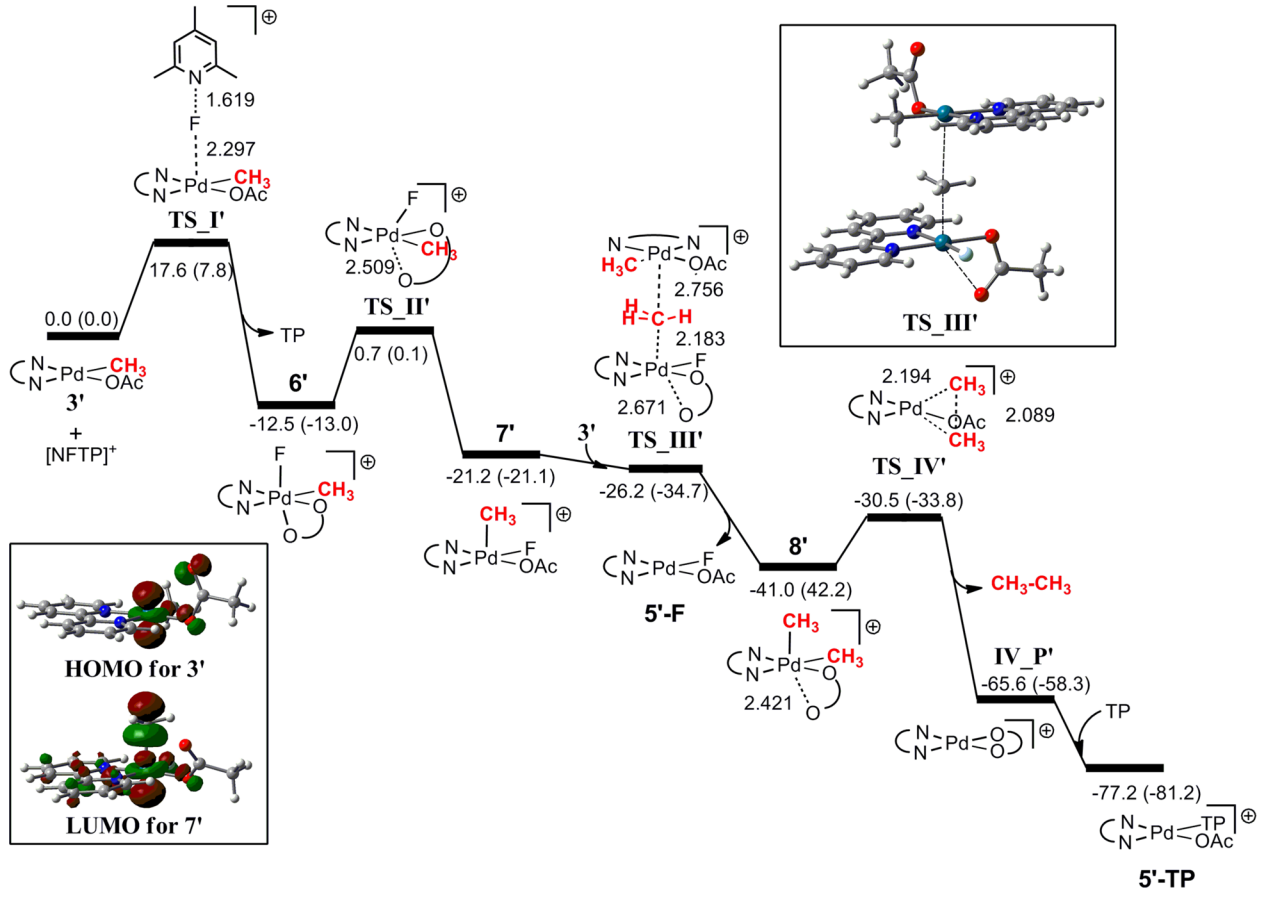

Figure 1. Energy profile for the reaction of (bpy)Pd(CH_3)(CF_3) (**3′**) with the *N*-fluoropyridinium cation, together with views of the HOMO for **3′** and LUMO for **7′**. TP = 2,4,6-trimethylpyridine. Energies ΔG (ΔH) in kcal/mol.

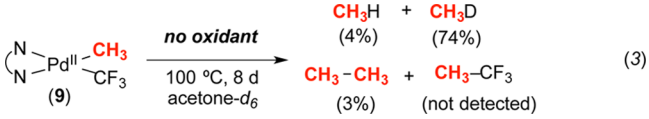

(3)

Table 3. Reaction of 9 with $AcFcBF_4$ and NFTPT[a]

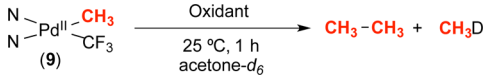

entry	oxidant	conditions	yield C_2H_6	yield CH_4
1	$AcFcBF_4$	none	34%	2%
2	NFTPT	none	41%	<1%
3[b]	$AcFcBF_4$	CHD	29%	2%
4[b]	NFTPT	CHD	42%	2%
5[c]	$AcFcBF_4$	no light	39%	<1%
6[c]	NFTPT	no light	42%	<1%

[a]Conditions: **9** (4 μmol, 1 equiv), $AcFcBF_4$ (4.8 μmol, 1.2 equiv) or NFTPT (20 μmol, 5 equiv), 1,1,2-trichloroethane (4 μmol, 1 equiv, standard), acetone-d_6, 25 °C, 1 h. [b]40 mmol of 1,4-cyclohexadiene (CHD) added under otherwise standard conditions. [c]Reaction conducted under standard conditions but in a foil-wrapped NMR tube to exclude ambient light.

byproduct of both of these reactions is (dtbpy)$Pd^{II}(CF_3)(X)^+$ (**10**, X = solvent, F^-, or TP), which is formed in 95 and 72% yield, respectively.[22] The reactions of **9** with $AcFcBF_4$ and NFTPT were essentially unaffected by the presence of 40 equiv of 1,4-cyclohexadiene (CHD, entries 3 and 4) and by the exclusion of light (entries 5 and 6). As with **3**, these results suggest against CH_3• intermediates as a major pathway to ethane formation.

DFT calculations show that the lowest energy path for the reaction of **9′** (bipyridine analogue of **9**) with NFTP is directly analogous to that for **3**. It involves three steps: (1) oxidation of 0.5 equiv of **9′** by NFTP to generate Pd^{IV} isomers **11′** and **12′**, (2) methyl group transmetalation between 1 equiv of **12′** and 1 equiv of Pd^{II} starting material **9′** to form **13′**,[23−25] and (3) ethane reductive elimination from **13′** to release the products (Scheme 4).[26] This sequence directly parallels that found for **3′** (Figure 1); as a result, most of the details are discussed in the Supporting Information. The barrier for

Scheme 4. Proposed Mechanism of Reaction of 9 with NFTPT

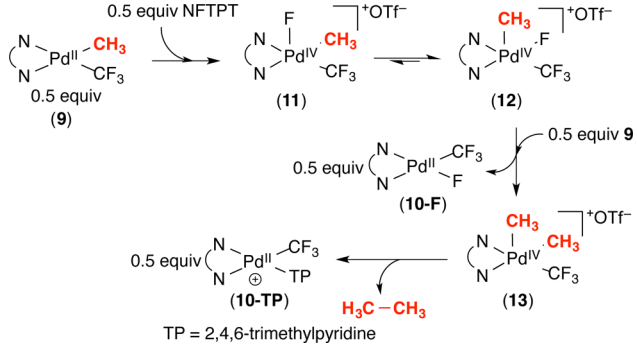

dx.doi.org/10.1021/ja412338k | J. Am. Chem. Soc. XXXX, XXX, XXX−XXX

ethane reductive elimination from **13′** is computed to be lower than that from **8′** (6.0 vs 10.5 kcal/mol, respectively). This difference can be attributed to the second weak C-O interaction in **8′**; generally, reductive elimination from six-coordinate complexes is slower than that from five-coordinate complexes.[27]

The DFT calculations suggest that intermediates **11**, **12**, and **13** should not be detectable, since the oxidation step has the highest barrier. However, we hypothesized that the addition of a coordinating solvent might trap **11**, **12**, and/or **13** as six-coordinate cationic species that could be detected at low temperature by NMR spectroscopy. Conducting the reaction of **9** with NFTPT at −40 °C in CD_2Cl_2 in the presence of 100 equiv of CD_3CN resulted in a complex and uninterpretable mixture of ^1H and ^{19}F NMR signals.[28] However, under otherwise identical conditions, the reaction of 1 equiv of **9** with 1.2 equiv of $AcFc^+$ afforded an intermediate with ^1H and ^{19}F NMR signals consistent with formulation as complex **13-CD_3CN** (Scheme 5).

Scheme 5. Reaction of 9 with $AcFc^+$ with Added CD_3CN

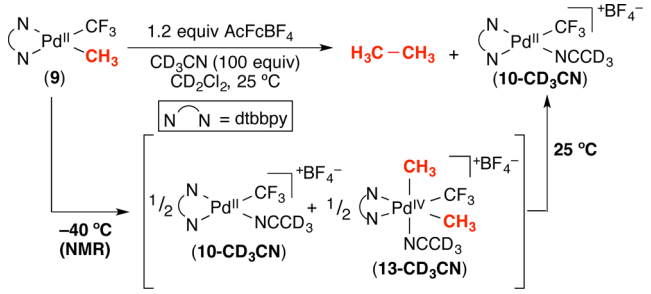

This species was formed in 28% yield relative to an internal standard along with 38% of the Pd^{II} product **10**. Warming the reaction mixture to 25 °C over 24 h resulted in disappearance of **13-CD_3CN**, with concomitant formation of ethane. Importantly, the rate of appearance of H_3C-CH_3 was identical to the rate of decay of **13-CD_3CN**.

We further corroborated the structure of **13-CD_3CN** by generating this complex *in situ* via an alternative route. The treatment of $(dtbpy)Pd(CH_3)_2$ (**1**) with CF_3^+ oxidant **14** at −40 °C afforded an intermediate with ^1H and ^{19}F NMR resonances matching those of putative intermediate **13-CD_3CN** (eq 4).[29] This observation, along with the DFT calculations, supports the involvement of Pd^{IV} intermediate **13-CD_3CN** in the oxidatively induced generation of ethane from **9**.

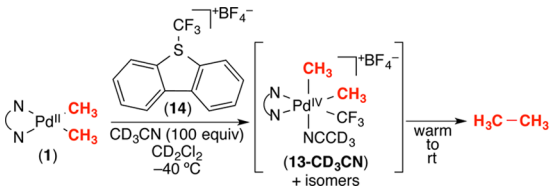

(4)

CONCLUSIONS

In summary, this report describes the oxidatively induced generation of H_3C-CH_3 from mono-methyl Pd^{II} acetate and trifluoromethyl complexes. Experimental studies suggest that the major pathway for ethane formation *does not* involve $CH_3\bullet$ intermediates. DFT calculations on the reaction of the OAc and CF_3 systems with NFTP show a low energy pathway involving methyl group transmetalation between 1 equiv of a Pd^{IV} intermediate and 1 equiv of the Pd^{II} starting material. The key Pd^{IV} dimethyl intermediate was detected and characterized during the reaction of $(dtbpy)Pd(CH_3)(CF_3)$ with $AcFcBF_4$. Overall, these transformations provide exciting precedent for the possibility of achieving C−C coupling of methane via a catalytic cycle like that in Scheme 2. Studies toward this goal are currently underway.

ASSOCIATED CONTENT

Supporting Information

Experimental and spectral details for all new compounds and all reactions reported. This material is available free of charge via the Internet at http://pubs.acs.org.

AUTHOR INFORMATION

Corresponding Authors

mssanfor@umich.edu
Allan.Canty@utas.edu.au

Notes

The authors declare no competing financial interest.

ACKNOWLEDGMENTS

This work was supported by NSF under the CCI Center for Enabling New Technologies through Catalysis (CENTC) Phase II Renewal, CHE-1205189, and the Australian Research Council.

REFERENCES

(1) (a) Crabtree, R. H. *Chem. Rev.* **1995**, *95*, 987. (b) Lunsford, J. H. *Angew. Chem., Int. Ed.* **1995**, *34*, 970. (c) Holmen, A. *Catal. Today* **2009**, *142*, 2. (d) Alvarez-Galvan, M. C.; Moto, N.; Ojeda, M.; Rojas, S.; Navarro, R. M.; Fierro, J. L. G. *Catal. Today* **2011**, *171*, 15. (e) Hammond, C.; Conrad, S.; Hermans, I. *ChemSusChem* **2012**, *5*, 1668.

(2) Examples: (a) Keller, G. E.; Bhasin, M. M. *J. Catal.* **1982**, *73*, 9. (b) Ito, T.; Lunsford, J. H. *Nature* **1985**, *314*, 721. (c) Chen, F.; Zheng, W.; Zhu, N.; Cheng, D.-G.; Zhan, X. *Catal. Lett.* **2008**, *125*, 348. (d) Liu, H.; Wei, Y.; Caro, J.; Wang, H. *ChemCatChem* **2010**, *2*, 1539. (e) Zavyalova, U.; Holena, M.; Schlogl, R.; Baerns, M. *ChemCatChem* **2011**, *3*, 1935.

(3) (a) Lanci, M. P.; Remy, M. S.; Kaminsky, W.; Mayer, J. M.; Sanford, M. S. *J. Am. Chem. Soc.* **2009**, *131*, 15618. (b) Lanci, M. P.; Remy, M. S.; Lao, D. B.; Sanford, M. S.; Mayer, J. M. *Organometallics* **2011**, *30*, 3704. (c) Khusnutdinova, J. R.; Rath, N. R.; Mirica, L. M. *J. Am. Chem. Soc.* **2012**, *134*, 2414.

(4) Examples of sp^3-C−H/sp^3-C−H coupling: (a) Li, Z.; Li, C.-J. *J. Am. Chem. Soc.* **2005**, *127*, 3672. (b) Li, Z.; Li, C.-J. *J. Am. Chem. Soc.* **2006**, *128*, 56. (c) Xie, J.; Li, H.; Zhou, I.; Cheng, Y.; Zhu, C. *Angew. Chem., Int. Ed.* **2012**, *51*, 1252. (d) Nobuta, T.; Tada, N.; Fujiya, A.; Kariya, A.; Miura, T.; Itoh, A. *Org. Lett.* **2013**, *15*, 574.

(5) Pd-mediated coupling of CH_4 to form AcOH: Periana, R. A.; Mironov, O.; Taube, D.; Bhalla, G.; Jones, C. J. *Science* **2003**, *301*, 814.

(6) Yeung, C. S.; Dong, V. M. *Chem. Rev.* **2011**, *111*, 1215.

(7) (a) Itatani, H.; Yoshimoto, H.; Shiotani, A.; Yokota, A.; Yoshikiyo, M. U.S. Patent 4,294,976, 1981. (b) Shiotani, A.; Itatani, H.; Inagaki, T. *J. Mol. Catal.* **1986**, *34*, 57.

(8) (a) Shilov, A. E.; Shul'pin, G. B. *Chem. Rev.* **1997**, *97*, 2879. (b) Stahl, S. S.; Labinger, J. A.; Bercaw, J. E. *Angew. Chem., Int. Ed.* **1998**, *37*, 2180. (c) Crabtree, R. H. *Dalton Trans.* **2001**, 2437. (d) Labinger, J. A.; Bercaw, J. E. *Nature* **2002**, *417*, 507. (e) Shul'pin, G. B. *Dalton Trans.* **2013**, *42*, 12794.

(9) Key examples: (a) Kao, L. C.; Hutson, A. C.; Sen, A. *J. Am. Chem. Soc.* **1991**, *113*, 700. (b) Muehlhofer, M.; Strassner, T.; Herrmann, W. A. *Angew. Chem., Int. Ed.* **2002**, *41*, 1745.

(10) For the generation of ethane from a Pd^{III} mono-methyl complex, see: (a) Khusnutdinova, J. R.; Rath, N. P.; Mirica, L. M.

dx.doi.org/10.1021/ja412338k | *J. Am. Chem. Soc.* XXXX, XXX, XXX−XXX

J. Am. Chem. Soc. **2010**, *132*, 7303. (b) Luo, J.; Rath, N. P.; Mirica, L. M. *Organometallics* **2013**, *32*, 3343.
(11) Remy, M. S.; Cundari, T.; Sanford, M. S. *Organometallics* **2010**, *29*, 1522.
(12) CH_3-CH_3 coupling at Pd^{IV}: (a) Byers, P. K.; Canty, A. J.; Skelton, B. W.; White, A. H. *J. Chem. Soc., Chem. Commun.* **1986**, 1722. (b) Byers, P. K.; Canty, A. J.; Crespo, M.; Puddephatt, R. J.; Scott, J. D. *Organometallics* **1988**, *7*, 1363. (c) Dücker-Benefer, C.; van Eldik, R.; Canty, A. J. *Organometallics* **1994**, *13*, 2412. (d) Canty, A. J. *Dalton Trans.* **2009**, 10409.
(13) CH_3-CH_3 coupling at Pd^{III}: (a) Khusnutdinova, J. R.; Qu, F.; Zhang, Y.; Rath, N. P.; Mirica, L. M. *Organometallics* **2012**, *31*, 4627. (b) Tang, F.; Zhang, Y.; Rath, N. P.; Mirica, L. M. *Organometallics* **2012**, *31*, 6690.
(14) Holtcamp, M. W.; Henling, L. M.; Day, M. W.; Labinger, J. A.; Bercaw, J. E. *Inorg. Chim. Acta* **1998**, *270*, 467.
(15) (a) Lin, M.; Hogan, T.; Sen, A. *J. Am. Chem. Soc.* **1997**, *119*, 6048. (b) An, Z.; Pan, X.; Liu, X.; Han, X.; Bao, X. *J. Am. Chem. Soc.* **2006**, *128*, 16028. (c) Yuan, J.; Wang, L.; Wang, L. *Ind. Eng. Chem. Res.* **2011**, *50*, 6513. (d) Munz, D.; Meyer, D.; Strassner, T. *Organometallics* **2013**, *32*, 3469. (e) Yuan, J.; Wang, Y.; Hao, C. *Catal. Lett.* **2013**, *143*, 610.
(16) (a) Siegbahn, P. E. M.; Crabtree, R. H.; Norlund, P. *J. Biol. Inorg. Chem.* **1998**, *3*, 314. (b) Garcia-Cuadrado, D.; Braga, A. A. C.; Maseras, F.; Echavarren, A. M. *J. Am. Chem. Soc.* **2006**, *128*, 1066. (c) Lafrance, M.; Fagnou, K. *J. Am. Chem. Soc.* **2006**, *128*, 16496. (d) Lafrance, M.; Gorelsky, S. I.; Fagnou, K. *J. Am. Chem. Soc.* **2007**, *129*, 14570. (e) Gorelsky, S. I.; Lapointe, D.; Fagnou, K. *J. Am. Chem. Soc.* **2008**, *130*, 10848. (f) Lapointe, D.; Fagnou, K. *Chem. Lett.* **2010**, *39*, 1118. (g) Sun, H.-Y.; Gorelsky, S. I.; Stuart, D. R.; Campeau, L.-C.; Fagnou, K. *J. Org. Chem.* **2010**, *75*, 8180. (h) Gorelsky, S.; Lapointe, D.; Fagnou, K. *J. Org. Chem.* **2012**, *77*, 658. (i) Maleckis, A.; Kampf, J. W.; Sanford, M. S. *J. Am. Chem. Soc.* **2013**, *135*, 6618.
(17) $AcFcBF_4$ provided higher yields than $FcBF_4$. The former is well-documented to be a stronger oxidant: Connelly, N. G.; Geiger, W. E. *Chem. Rev.* **1996**, *96*, 877.
(18) (a) Hull, K. L.; Anani, W. Q.; Sanford, M. S. *J. Am. Chem. Soc.* **2006**, *128*, 7134. (b) Ball, N. D.; Kampf, J. W.; Sanford, M. S. *J. Am. Chem. Soc.* **2010**, *132*, 2878. (c) Racowski, J. M.; Ball, N. D.; Sanford, M. S. *J. Am. Chem. Soc.* **2011**, *133*, 18022. (d) Racowski, J. M.; Gary, J. B.; Sanford, M. S. *Angew. Chem., Int. Ed.* **2012**, *51*, 3414. (e) Maleckis, A.; Sanford, M. S. *Organometallics* **2011**, *30*, 6617.
(19) The initial oxidation of Pd^{II} with $AcFcBF_4$ almost certainly occurs via an outer sphere $1e^-$ pathway, and the resulting open shell intermediate(s) are very challenging to assess computationally. However, our prior studies of the reactivity of **1** with Fc^+ show that $1e^-$ oxidants can ultimately yield Pd^{IV} intermediates (i.e., **2**) via methyl group transmetalation and a second $1e^-$ oxidation. (Importantly, these latter two steps could occur in either order, with CH_3 group transmetalation occurring at either Pd^{III} or Pd^{IV}; see refs 23−25 for examples of each possibility.) These results suggest that it is reasonable that ethane formation from **3** with $AcFcBF_4$ and NFTPT could proceed via an analogous penultimate Pd^{IV} intermediate (**8**).
(20) Gaussian 09 was used at the B3LYP level for geometry optimization with dichloromethane as solvent utilizing the SDD basis set on Pd and the 6-31G(d) basis set for other atoms. Single point energy calculations for all structures at the M06 level employed the quadrupole-ξ valence def2-QZVP basis set on Pd along with the corresponding ECP and the 6-311+G(2d,p) basis set on other atoms. See the Supporting Information for full details.
(21) (a) Ye, Y.; Ball, N. D.; Kampf, J. W.; Sanford, M. S. *J. Am. Chem. Soc.* **2010**, *132*, 14682. (b) Powers, D. C.; Lee, E.; Ariafard, A.; Sanford, M. S.; Yates, B. F.; Canty, A. J.; Ritter, T. *J. Am. Chem. Soc.* **2012**, *134*, 12002.
(22) The X ligands of **10** (BF_4, F, and TP) are in rapid exchange with solvent (acetone or water); thus, the complexes were converted to the corresponding iodide salts to determine yields.
(23) Pd^{IV} to Pd^{II} methyl group transmetalation: (a) Markies, B. A.; Canty, A. J.; Boersma, J.; van Koten, G. *Organometallics* **1994**, *13*, 2053. (b) Kruis, D.; Markies, B. A.; Canty, A. J.; Boersma, J.; van Koten, G. *J. Organomet. Chem.* **1997**, *532*, 235. (c) Canty, A. J.; Denney, M. C.; Skelton, B. W.; White, A. H. *Organometallics* **2004**, *23*, 1122. (d) Canty, A. J.; Rodemann, T.; Ryan, J. H.; Skelton, B. W.; White, A. H. *Organometallics* **2004**, *23*, 3466.
(24) Pd^{IV} to Pt^{II} methyl group transmetalation, including kinetics: Aye, K.-T.; Canty, A. J.; Crespo, M.; Puddephatt, R. J.; Scott, J. D.; Watson, A. A. *Organometallics* **1989**, *8*, 1518.
(25) Related reactions at Pt^{III} and Pt^{IV}: (a) Wang, L.; Stahl, S. S.; Labinger, J. A.; Bercaw, J. E. *J. Mol. Catal. A: Chem.* **1997**, *116*, 269. (b) Johansson, L.; Ryan, O. B.; Romming, C.; Tilset, M. *Organometallics* **1998**, *17*, 3957.
(26) On the basis of logic analogous to that in ref 19, we believe that it is reasonable to propose that the oxidation of **9** with NFTPT and $AcFcBF_4$ likely proceed via the same penultimate Pd^{IV} intermediate **13**.
(27) (a) Bartlett, K. L.; Goldberg, K. I.; Borden, W. T. *J. Am. Chem. Soc.* **2000**, *122*, 1456. (b) Crumpton, D. M.; Goldberg, K. I. *J. Am. Chem. Soc.* **2000**, *122*, 962.
(28) The complex mixtures of intermediates observed with NFTPT are likely due to the presence of two potential counterions (F and OTf) as well as two potential L-type ligands (solvent and 2,4,6-trimethylpyridine) in this system.
(29) The expected organic byproduct benzothiophene was formed in 39% NMR yield at the end of this reaction.